Pergamon

Int. J. Heat Mass Transfer. Vol. 41, No. 2, pp. 313–322, 1998

Printed in Great Britain
0017–9310/98 $19.00+0.00

PII: S0017–9310(97)00135–X

Application of experimental design methods to assess the effect of uncertain boundary conditions in inverse heat transfer problems

PAMELA M. NORRIS

Department of Mechanical, Aerospace and Nuclear Engineering, University of Virginia, Charlottesville, VA 22903, U.S.A.

(*Received* 26 *April* 1996 *and in final form* 6 *May* 1997)

Abstract—Inverse methods are often used in heat transfer analysis to determine parameters which are difficult or impossible to measure directly, from carefully selected experimental measurements which can be more easily carried out. In this type of procedure, there are often a large number of boundary conditions which can affect the outcome. Often it is impractical, or even impossible, to accurately measure all influential boundary conditions, and thus estimates are employed. However, the question naturally arises, how sensitive are the results of the inverse analysis to the assumed boundary conditions? A statistical method, employing an orthogonal array matrix designed experiment, which was used to estimate the effect of the uncertain boundary conditions on the results of the analysis, is described in detail and the results are given.

1. INTRODUCTION

A statistical procedure is presented which can be used to assess the effect of uncertain boundary conditions in inverse heat transfer problems. The need for this procedure grew from previous research efforts in which it was desired to identify the heat transfer regimes present in the coolant passages of a diesel engine cylinder head. This investigation involved a side-by-side analytical and experimental investigation. A series of experiments was performed, and the temperatures at several locations inside the cylinder head of a fully functioning engine were measured. A finite element model of the cylinder head geometry was developed using ANSYS®. The convection coefficients along the coolant flow passages were determined by adjusting the assumed values until the finite element model reproduced the experimental temperature field results. Values for all the other boundary conditions required for this model were identified either by direct measurement or by estimation based on historical data. It is the sensitivity of the results of the finite element analysis, and hence the sensitivity of the parameters determined from the inverse analysis, to these imprecise boundary conditions that is addressed here in detail. The heat transfer study will be briefly presented first and then the application of the statistical procedure to this particular example will be discussed. Additional information about the engine heat transfer study can be found in Norris [1], Norris *et al.* [2, 3].

2. HEAT TRANSFER STUDY

The original project was motivated by the need to better understand the fundamentals of heat transfer in diesel engine cylinder heads. The goal of the investigation was to identify the heat transfer regimes present in the valve bridge coolant passages of a diesel engine cylinder head. Past studies have demonstrated that both nucleate and film boiling can occur in the cooling jackets of an engine [4]. Nucleate boiling may be desirable, as heat transfer in this regime is very efficient because as the bubbles grow and are carried into the mainstream of the liquid, they disturb the boundary layer and increase mixing. As the intensity of nucleate boiling increases, the heat flux rises rapidly with little increase in surface temperature. However, at sufficiently high wall temperatures, transition or partial film boiling occurs. In this regime bubbles are forming so rapidly that a continuous vapor film forms on the surface and conditions may oscillate between film and nucleate boiling. If transition boiling occurs, which would be accompanied by a decrease in the heat transfer coefficient, local hot spots can occur and adversely affect the fatigue life of the cylinder head, resulting in eventual cylinder head failure.

For this investigation experimental results were used in conjunction with a finite element model to identify the heat transfer coefficients along the coolant flow passages in a Cummins Engine Co., Inc. L10 cylinder head. Since the convective heat transfer coefficients were not known *a priori*, the analysis required an iterative procedure. The side by side analytical/experimental analysis is depicted in the flowchart in Fig. 1. A series of experiments was performed, and the temperatures at several locations in a fully functioning engine were measured by means of embedded thermocouples. A three-dimensional finite element model of a portion of the cylinder head geometry was developed using ANSYS®. Values for

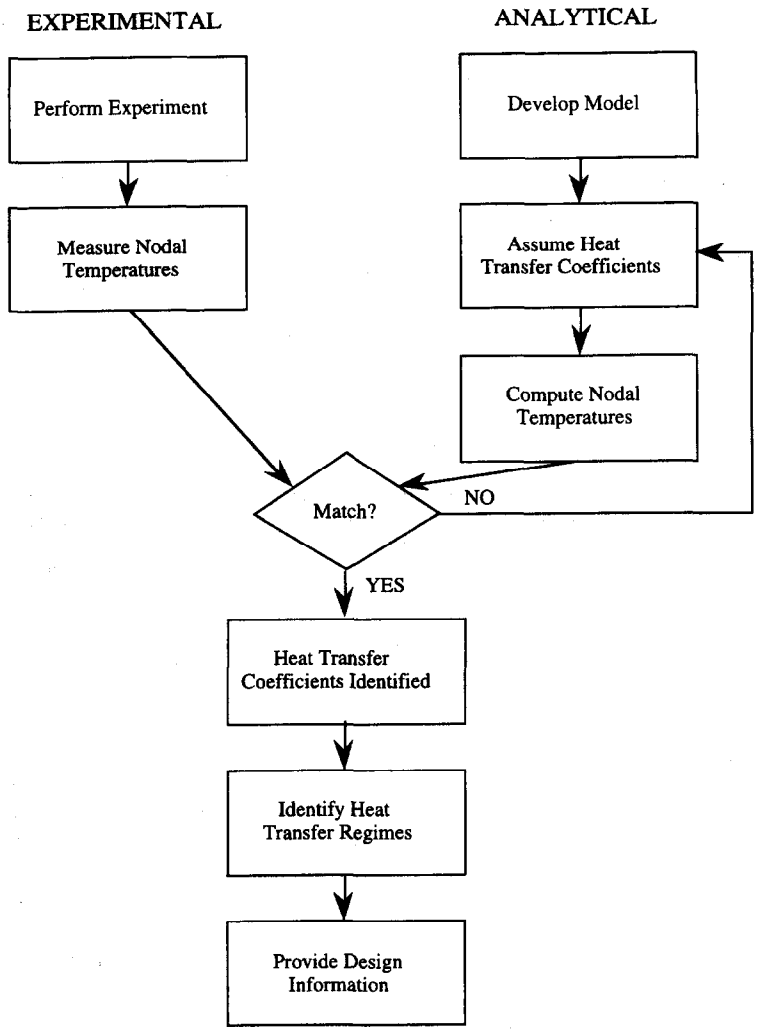

Fig. 1. Analytical/experimental procedure.

the heat transfer coefficients along the coolant flow passages were assumed, and the resulting temperature profile in the cylinder head was computed. The assumed heat transfer coefficients were then adjusted until the finite element model reproduced the experimental temperature results. During this iterative procedure the coefficients were manually adjusted making use of the assumption that the temperature at each thermocouple location was affected solely by the assumed convection coefficient for the region in which the thermocouple was located. The validity of this assumption will be discussed in Section 3.4. The iterative procedure continued until the convection coefficients which enabled the finite element model to reproduce the experimental results (to four significant figures) were identified (to three significant figures). In this manner the heat transfer coefficients along the coolant flow passages were determined, and in turn were used to identify the heat transfer regimes present in the valve bridge coolant passages. The analysis confirmed that local nucleate boiling is present in several locations in the L10 cylinder head and identified locations where transition boiling may occur.

2.1. *Flow paths and thermocouple locations*

Figure 2 shows the coolant flow paths through the lower cooling jacket of the L10 head as revealed during a flow visualization study using a full-scale transparent model of the L10 cylinder head [5]. This figure shows three cylinders of the six cylinder head. The flow

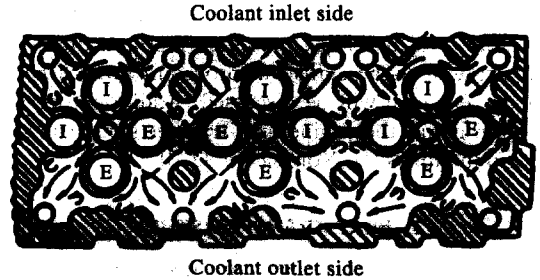

Fig. 2. Coolant flow paths.

passages in the L10 are divided into two symmetric halves; hence the study concentrated on three cylinders. Note in this figure the alternating placement of the exhaust and intake valves, indicated in the figure by E and I, respectively.

Figure 3 details the flow in the valve bridge region as revealed by the flow visualization study [5]. The coolant enters the 'upstream' valve bridges and flows around the injector and through the 'downstream' bridges. A near zero velocity region, indicated in the figure as 'stagnation,' was observed on both the upstream and downstream sides of the injector sleeve. As the coolant entered the downstream valve bridges it was observed to separate from the jacket wall, leaving a recirculating zone adjacent to the wall. This is also shown in Fig. 3. These two regions were cause for concern, as both are in high heat flux regions where adequate cooling is imperative to prevent local hot spots which would adversely affect the fatigue life of the cylinder head. A final region of concern is that seen in Fig. 2, between any two cylinders. On both the upstream and downstream sides a recirculation region exists. On cylinders having adjacent exhaust ports, such as the left two cylinders in Fig. 2, this too is a region of high heat flux.

The results of the flow visualization study were used to identify distinct flow zones within the cylinder head. Velocity estimates were made for each zone based on the flow visualization study and Gnielineski's convection correlation was used to obtain estimates for the heat transfer coefficients, assuming all heat transfer occurred by pure convection [6]. These estimates were considered satisfactory for the areas where the flow appeared steady, but were highly uncertain for the four areas identified in which details of the flow are uncertain due to the possibility of boundary layer separation, recirculation, and stagnation. The primary goal of this analysis was to determine the heat transfer coefficients for these four critical flow zones: the apparently stagnant region at the injector bore, the separation region in the downstream valve bridge, the recirculation region between cylinders on the downstream side, and the recirculation region between cylinders on the upstream side. This was accomplished by using the iterative procedure depicted in Fig. 1.

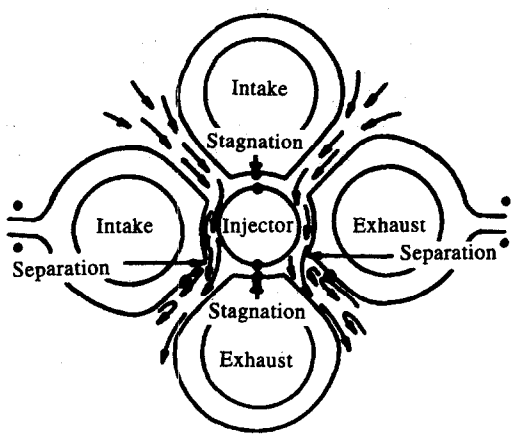

Fig. 3. Flow details in valve bridge area.

To investigate the presence of boiling in the coolant passages, three of the six cylinders in the head were instrumented with small diameter thermocouples, one in each of the critical flow areas. The thermocouple locations for cylinder one (an end cylinder) are shown in Fig. 3 (indicated by dots), along with results of the flow visualization study. The thermocouples were skillfully embedded such that the thermocouple bead is positioned just on the lower coolant passage wall. The precise thermocouple locations were largely dictated by ease of installation. It is assumed that these beads do not interfere significantly with the coolant flow or the boundary layer.

2.2. *Analytical model and boundary conditions*

A study conducted at Komatsu Ltd indicated that the results from a finite element analysis using only the portion of the head between the flame face and the coolant passages around one intake and one exhaust port were identical to those using an entire cylinder [7]. This has also been illustrated in unpublished studies by Cummins. Therefore, only the portion of the L10 cylinder head from the flame face up to about the midpoint of the coolant passages (called the fire-deck) for one-half of one cylinder was modeled. The portions modeled are shown, indicated by the dotted lines, in Fig. 2, as seen from the flame face. The same geometric model may be used for any pair of intake and exhaust valves for any of the cylinders. It is assumed that the heat flow is symmetric about the center line.

The results of the finite element model depend strongly on the 15 boundary conditions listed in Table 1. For this study the thermal load was assumed constant since the cylinder head temperatures cannot rise or fall appreciably in the short time over which one cycle occurs. Most of the recorded data for the L10 engine is at the rated condition for the engine (1800 rpm and 270 hp). Therefore, the analysis concentrated on the rated condition and represented a worst case. Of these 15 boundary conditions, only one, the injector sleeve temperature, was directly measured during the experiment. Additionally, the bulk fluid temperature was indirectly measured, and the temperature of the intake air was measured at the entrance to the intake manifold. However, the temperature rises as the air travels through the intake port, and based on past experience, the average intake air temperature was assumed to be equal to the measured temperature plus 10 degrees. Estimates for the remaining 12 boundary conditions were obtained making use of an extensive historical data base developed for the L10 engine. It should be noted that the convection coefficient on the flame face, H_{fac}, was not specified as a single value, but rather as a detailed profile which resulted from extensive experimentation at Cummins. This profile will simply be referred to as H_{fac}.

Table 1. Experimental factors (boundary conditions) and the assigned levels

Column (factor) number and description	Symbol (units)		Factor levels 1 (low)	2 (nominal)	3 (high)
1 Convective heat transfer coefficient into engine block	H_{blo}	(kW m^{-2} K^{-1})	4.09		7.36
2 Convective heat transfer coefficient into intake valve	H_{int}	(kW m^{-2} K^{-1})	1.23		4.09
3 Empty					
4 Convective heat transfer coefficient on flame face	H_{fac}	(kW m^{-2} K^{-1})	0.8*Nom	Nom	1.2*Nom
5 Convective heat transfer coefficient inside exhaust port	H_{gas}	(kW m^{-2} K^{-1})	0.409	0.531	0.653
6 Temperature of exhaust gases	T_{gas}	(K)	700	839	978
7 Convective heat transfer coefficient into exhaust valve	H_{exh}	(kW m^{-2} K^{-1})	1.23	2.86	4.50
8 Average temperature of exhaust valve	T_{exh}	(K)	700	811	922
9 Convection heat transfer coefficient inside intake port	H_{air}	(kW m^{-2} K^{-1})	0.164	0.286	0.408
10 Temperature of intake air in intake port	T_{air}	(K)	317	325	333
11 Temperature of engine block	T_{blo}	(K)	355	375	395
12 Average temperature of intake valve	T_{int}	(K)	533	672	811
13 Convection coefficient into portion not modeled	H_{equ}	(kW m^{-2} K^{-1})	8.18×10^{-7}	8.18×10^{-5}	8.18×10^{-3}
14 Bulk fluid temperature	T_{flu}	(K)	350	355	360
15 Temperature of combustion gases on flame face	T_{fac}	(K)	922	1089	1256
16 Copper fuel injector sleeve temperature	T_{inj}	(K)	350	358	366

2.3. *Preliminary results*

Table 2 lists the heat transfer coefficients calculated by using velocity estimates obtained during the flow visualization study along with a pure convection heat transfer correlation, as well as the heat transfer coefficients determined from the iterative procedure for the four regions of interest for all three cylinders. Due to the alternating placement of valves, the modeled areas in cylinders 2 and 3 overlap in the recirculation regions between cylinders. Hence, the convection coefficients identified for these regions in cylinders 2 and 3 should be nearly identical. As seen in Table 2, when the finite element model for cylinder 2 is used along with the appropriate experimental data and boundary conditions, the heat transfer coefficients identified for the downstream and upstream recirculation regions were 6.58 and 47.9 kW m^{-2} K^{-1}, respectively. Similarly, the values identified for cylinder 3, using the appropriate experimental data and boundary conditions for this cylinder, were 6.60 and 48.0 kW m^{-2} K^{-1}, respectively. This close agreement helps confirm the validity of the analysis.

By examining the data listed in Table 2 several conclusions may be drawn. In the separation region in the downstream valve bridge, the calculated heat transfer coefficient in all three cylinders is much higher than that estimated for pure convection. Hence, the dominant mechanism of heat transfer in this separation region is nucleate boiling. The results for the region believed to be stagnant at the injector bore are very similar and nucleate boiling appears to be the dominant mechanism of heat transfer in all three cylinders. Thus, even in this region, where the earlier flow visualization studies indicated little or no fluid velocity, there is no evidence of dryout. This strongly suggests that a sufficient fluid flow is maintained in this area to provide effective cooling. This fluid flow may be caused by engine vibrations or by fluid temperature gradients, which would not have been observed in the flow visualization studies [2].

In the recirculation region between cylinders on the downstream side, the results for cylinder 1 are considerably different from those for cylinders 2 and 3. The calculated coefficient for cylinder 1 is high enough to suggest a small amount of nucleate boiling, however, the low coefficient calculated for the downstream region between cylinders 2 and 3 suggests transition boiling. These results are consistent with the fact that the end cylinder runs considerably cooler than the inner cylinders. Thus the inner cylinders may

Table 2. Heat transfer coefficients (kW m^{-2} K^{-1})

Region	Pure convection	Cylinder 1	Cylinder 2	Cylinder 3
Separation	16	528	71.3	406
Downstream recirculation	25	59.8	6.58	6.60
Upstream recirculation	29	236	47.9	48.0
Stagnant	8	384	386	199

Note: proceeding decimal point indicates all digits are significant.

be hot enough to support a transition from the nucleate to the transition boiling regime. In the recirculation region between cylinders on the upstream side, the results do not support a firm conclusion. It appears, however, that nucleate boiling is present in all three cylinders in this region.

This analysis indicated that local nucleate boiling occurs at several locations in the L10 head and that transition boiling may occur in the recirculation region between interior cylinders on the downstream side. Studies on cracked heads have indicated that all bridge failures occur in the interior cylinders of the in-line six cylinder L10 head, which agrees with the results of this analysis.

3. STATISTICAL SENSITIVITY ANALYSIS

At this point, since not all of the boundary conditions were measured experimentally, an analysis was conducted to determine the effect of uncertainty in the boundary conditions on the parameters determined from the inverse analysis. For example, if the average temperature of the intake valve had been estimated as 672 K, but was actually only 533 K, what effect would this have on the finite element model calculated temperatures and in turn on the convection coefficients identified from the analysis.

As listed in Table 1, there is a total of 15 boundary conditions which must be specified for the finite element procedure. The conventional approach would be to investigate the parameters in a 'one-factor-at-a-time' procedure. However, this method, in which experimental factors are varied one at a time, with the remaining factors held constant, only provides estimates of the effects of single variables at selected fixed levels of all other variables. It is then necessary to assume that the effect would be the same at different settings of the other variables [8]. Certainly this is not valid for the study given here. For example, the effect of changing the equivalent heat transfer coefficient into the intake valve will be much greater when the temperature of the intake valve is 672 K rather than 533 K.

To overcome this difficulty a factorial design could be used in which the investigator selects a fixed number of levels for each of the variables and then runs experiments with all possible combinations [8]. For this example, which has 15 variables, 225 experiments would be required even if each factor were investigated only at two levels. Of course this offers a huge savings over the one-factor-at-a-time approach which would require 1800 experiments to obtain the same precision, but 225 is still unmanageable.

To reduce the number of experiments required while still obtaining sufficient information to guide the experimenter, the author suggests the application of a matrix experiment using orthogonal arrays, a method commonly used in robust design. As will be demonstrated, only 36 experiments were necessary to investigate the effect of the 15 boundary conditions (13 at three levels and two at two levels). This method offers the additional advantage that, with the assumption that the superposition model approximately holds, i.e. that the total effect of the factors is equal to the sum of the individual factor effects, data reduction simply involves averaging and is very straight forward and easy to interpret.

3.1. *Theory*

The statistical sensitivity analysis began by identifying the range over which each of the boundary conditions may lie. Conservative upper and lower limits for each of the boundary conditions were identified based on scientific phenomena and past engineering experience, and the statistical region formed by these limits is the region of interest, also called the 'experimental' region. An orthogonal array matrix designed experiment was used to investigate the effect of all 15 boundary conditions, also called the experimental factors, simultaneously, and the estimated effect of each boundary condition is valid even when the other boundary conditions vary over the experimental region [9].

A matrix experiment consists of a set of experiments where the values (or levels) of the factors, here the boundary conditions, are changed from one experiment to another according to the experimental design matrix, which in this case is an orthogonal array. As the name suggests, the columns of an orthogonal array are mutually orthogonal—that is, for any pair of columns, all combinations of factor levels occur and they occur an equal number of times [9].

There are a limited number of standard orthogonal arrays, so it was necessary to force the desired experiment to fit an available array. Table 3 shows the experimental design matrix selected for this analysis. It is the standard Taguchi orthogonal array L'_{36} [10]. This matrix was selected because it most nearly matched the requirements of this analysis. The design matrix delineates the conditions for each of the experiments to be performed. The 36 rows represent the experiments (or runs) to be performed. The 16 columns of the matrix represent the 16 factors which may be investigated. The entries in the design matrix (the 1s, 2s and 3s) indicate the levels of the factors.

The factor levels chosen for this analysis are given in Table 1. The low level has arbitrarily been labeled '1', the nominal level '2', and the high level '3'. The high and low levels correspond to the upper and lower limits identified for each boundary condition, and the nominal level, which is actually the best estimate available for each factor, is between these limits. Since there are only fifteen boundary conditions, one column will remain empty; this will not affect the orthogonality of the design [9]. The 15 factors are assigned column numbers as also indicated in Table 1. In this design matrix the first three variables have only two levels while the remaining thirteen variables have three. Therefore, the variables selected to be assigned to the first two columns were those that are not believed to

Table 3. Experimental design matrix and sample observations

Exp #\Factor #	1	2	3	4	5	6	7	8	9	10	11	12	13	14	15	16	Observation
1	1	1	1	1	1	1	1	1	1	1	1	1	1	1	1	1	350.72 K
2	1	1	1	1	2	2	2	2	2	2	2	2	2	2	2	2	359.51 K
3	1	1	1	1	3	3	3	3	3	3	3	3	3	3	3	3	362.63 K
4	1	2	2	1	1	1	1	1	2	2	2	2	3	3	3	3	362.66 K
5	1	2	2	1	2	2	2	2	3	3	3	3	1	1	1	1	351.04 K
6	1	2	2	1	3	3	3	3	1	1	1	1	2	2	2	2	356.74 K
7	2	1	2	1	1	1	2	3	1	2	3	3	1	2	2	3	357.24 K
8	2	1	2	1	2	2	3	1	2	3	1	1	2	3	3	1	361.75 K
9	2	1	2	1	3	3	1	2	3	1	2	2	3	1	1	2	351.06 K
10	2	2	1	1	1	1	3	2	1	3	2	3	2	1	3	2	352.04 K
11	2	2	1	1	2	2	1	3	2	1	3	1	3	2	1	3	356.77 K
12	2	2	1	1	3	3	2	1	3	2	1	2	1	3	2	1	361.56 K
13	1	1	1	2	1	2	3	1	3	2	1	3	3	2	1	2	356.57 K
14	1	1	1	2	2	3	1	2	1	3	2	1	1	3	2	3	362.61 K
15	1	1	1	2	3	1	2	3	2	1	3	2	2	1	3	1	351.52 K
16	1	2	2	2	1	2	3	2	1	1	3	2	3	3	2	1	361.93 K
17	1	2	2	2	2	3	1	3	2	2	1	3	1	1	3	2	352.18 K
18	1	2	2	2	3	1	2	1	3	3	2	1	2	2	1	3	356.92 K
19	2	1	2	2	1	2	1	3	3	3	1	2	2	1	2	3	352.01 K
20	2	1	2	2	2	3	2	1	1	1	2	3	3	2	3	1	356.94 K
21	2	1	2	2	3	1	3	2	2	2	3	1	1	3	1	2	361.78 K
22	2	2	1	2	1	2	2	3	3	1	2	1	1	3	3	2	362.34 K
23	2	2	1	2	2	3	3	1	1	2	3	2	2	1	1	3	351.95 K
24	2	2	1	2	3	1	1	2	2	3	1	3	3	2	2	1	356.77 K
25	1	1	1	3	1	3	2	1	2	3	3	1	3	1	2	2	351.95 K
26	1	1	1	3	2	1	3	2	3	1	1	2	1	2	3	3	357.69 K
27	1	1	1	3	3	2	1	3	1	2	2	3	2	3	1	1	361.76 K
28	1	2	2	3	1	3	2	2	2	1	1	3	2	3	1	3	362.61 K
29	1	2	2	3	2	1	3	3	3	2	2	1	3	1	2	1	351.31 K
30	1	2	2	3	3	2	1	1	1	3	3	2	1	2	3	2	357.63 K
31	2	1	2	3	1	3	3	3	2	3	2	2	1	2	1	1	356.40 K
32	2	1	2	3	2	1	1	1	3	1	3	3	2	3	2	2	362.24 K
33	2	1	2	3	3	2	2	2	1	2	1	1	3	1	3	3	352.63 K
34	2	2	1	3	1	3	1	2	3	2	3	1	2	2	3	1	356.87 K
35	2	2	1	3	2	1	2	3	1	3	1	2	3	3	1	2	362.22 K
36	2	2	1	3	3	2	3	1	2	1	2	3	1	1	2	3	352.43 K

have large effects, and column number three was chosen as the empty column. For this analysis each experiment is one complete ANSYS® run utilizing the prescribed levels for each factor, i.e. the boundary conditions. For example, experiment one requires one complete run with the value for each factor set at the first level, the low level. For each 'experiment' the temperature at the four nodal points corresponding to the four thermocouple locations was recorded.

In this experimental design the effect of each of the 15 variables, called the main effects, can be determined independently, but it is not possible to distinguish any factor interactions from the main effects. This means that the following simple linear model is assumed for the response η:

$$\eta = \text{overall mean} + \sum_{\text{all factors}} (\text{factor effect}) + \text{error} \quad (1)$$

where error here implies the error of the additive approximation. Note, in typical design of experiments analysis the error term would include a contribution due to the error in the repeatability of measuring the response, η, for a given experiment. However, for the case presented here the response is calculated from the finite element analysis and thus this component of error does not exist. This model, also referred to as a superposition model, implies that the total effect of the factors is equal to the sum of the individual factor effects. This does not preclude the individual factor effects from being quadratic or higher-order, but does ignore the presence of any cross product terms involving two or more factors. Thus, factor interactions are ignored [9].

This sort of design is a saturated design, also called a Resolution III design. A saturated design results when a variable is assigned to each column of an array [9]. This experiment corresponds to the 'screening'

phase used in classical experimental design. In this phase Resolution III designs are used for studies with a large number of factors in order to determine the relative importance of each factor. The screening phase would normally be followed by a modeling phase. In the modeling phase a higher resolution design would be utilized which would allow for the estimation of interactions. In this phase those factors found important during the screening phase would be further investigated in order to build a mathematical model. Since the primary purpose of this analysis is to determine the effect of each boundary condition and to identify those with the largest effects, not to develop a model with which to predict temperatures, the modeling phase is not necessary and this saturated design is adequate.

3.2. *Analysis*

A complete finite element analysis was performed using each of the 36 sets of boundary conditions prescribed by the experimental design matrix. For each run the temperature at each of the four nodal points of interest was recorded. These temperatures are called the observations. As an example, the observations for the nodal point located at the thermocouple location in the stagnant region at the injector bore are listed in the last column of Table 3. The sample calculations which follow will be based on this data. Similar calculations were performed for the other three locations of interest and are shown in Norris [1], but are not shown here for the sake of brevity. The observations were then used to estimate the effect of each of the 15 variables on the temperatures at each of the four nodal points using a process sometimes called analysis of means, ANOM [9].

Using the temperatures recorded at each location for each of the 16 runs, the effect at that location for each level of the 15 variables was calculated. Let the recorded temperature, the observation, for each of the $i = 36$ runs at the location of interest be denoted by $\eta_i\,(i = 1, 36)$. The balanced overall mean temperature, over the entire experimental region is:

$$m = \left(\sum_{i=1}^{36} \eta_i\right)/36 = 357.02\,\text{K}. \tag{2}$$

The average temperature when the factor in column one, H_{blo}, is at the low level, denoted $m_{1\text{L}}$, is:

$$m_{1\text{L}} = \left(\sum_{i=1}^{6} \eta_i + \sum_{i=13}^{18} \eta_i + \sum_{i=25}^{30} \eta_i\right)/18 = 357.11\,\text{K}. \tag{3}$$

This average temperature is calculated using only results from runs in which H_{blo} was at the low level. Therefore, only results corresponding to the eighteen experiments with a '1' in the first column of the design matrix are used. Since an orthogonal array matrix design was used for this analysis, this average is balanced over all levels of the other 14 factors. The effect of a factor level is defined as the deviation it causes from the overall mean [9]. Thus, the effect of H_{blo} at the low level is given by

$$m_{1\text{L}} - m = 357.11\,\text{K} - 357.02\,\text{K} = 0.09\,\text{K}. \tag{4}$$

Similarly, the average temperature when H_{blo} is at the high level, denoted $m_{1\text{H}}$, was found to be 356.93 K, and thus the effect of H_{blo} at the high level is -0.09 K.

In a similar manner the average temperature when the factor in column four, H_{fac}, a three level factor, is at the low level, denoted $m_{4\text{L}}$, is found by,

$$m_{4\text{L}} = \left(\sum_{i=1}^{12} \eta_i\right)/12 = 356.98\,\text{K} \tag{5}$$

and thus, the effect of H_{fac} at the low level is

$$m_{4\text{L}} - m = 356.98\,\text{K} - 357.02\,\text{K} = -0.04\,\text{K}. \tag{6}$$

The average temperature for each level of the other 13 factors was calculated in a similar manner, and the resulting effects are listed in Table 4. This same procedure was used to calculate factor effects for the other three locations of interest, and the results can be found in Norris [1].

From Table 4, when the value of factor one, H_{blo}, is set at the low level, 4.09 kW m^{-2} K^{-1}, the average nodal temperature is 0.09 K higher than the overall average temperature. And when the value of H_{blo} is set at the high level, 7.36 kW m^{-2} K^{-1}, the average nodal temperature is 0.09 K lower than the overall average temperature. Thus, changing the value of H_{blo} from 4.09 kW m^{-2} K^{-1} to 7.36 kW m^{-2} K^{-1} causes the average nodal temperature to change by 0.18 K.

As can be seen in Table 4, each boundary condition and their different levels affect the calculated temperature to varying degrees. A better way to judge the relative importance of each of the boundary conditions on the overall mean temperature requires calculation of the sum of squares due to each factor. The sum of squares due to factor one, SS_1, is equal to the total squared deviation of the average at each level from the overall average temperature. There are 18 experiments each at the low and high levels of the factor in column one, H_{blo} (which is a two-level factor), therefore,

$$\begin{aligned} SS_1 &= 18(m_{1\text{L}} - m)^2 + 18(m_{1\text{H}} - m)^2 \\ &= 18(357.11 - 357.02)^2 + 18(356.94 - 357.02)^2 \\ &= 0.26. \end{aligned} \tag{7}$$

This statistic tells how the levels of H_{blo} influence the nodal temperature by using the average temperature at each level of H_{blo}, thus showing how much variation H_{blo} adds to the total variation [9].

Table 4. Factors in order of decreasing influence

Factor		Effects by level			Sum of squares (SS)	Contribution to SS_{Total} (%)
		Low	Nominal	High		
T_{flu}	Bulk fluid temp	−5.29	0.15	5.14	652.68	98.00
T_{inj}	Injector sleeve temp	−0.48	0.15	0.32	4.24	0.64
T_{fac}	Temp of gases on flame face	−0.37	0.17	0.21	2.51	0.38
H_{air}	Conv coeff inside intake port	0.01	0.17	−0.18	0.74	0.11
T_{exh}	Avg temp of exhaust valve	−0.08	0.19	−0.11	0.63	0.10
T_{int}	Avg temp of intake valve	−0.17	0.15	0.01	0.62	0.09
H_{exh}	Conv coeff into exhaust valve	−0.08	0.17	−0.09	0.54	0.08
T_{gas}	Temp of exhaust gases	−0.10	0.16	−0.07	0.49	0.07
H_{gas}	Conv coeff inside exhaust port	−0.09	0.16	−0.07	0.46	0.07
T_{air}	Temp of intake air	−0.12	0.14	−0.03	0.42	0.06
H_{equ}	Conv coeff into part not modeled	−0.06	0.14	−0.07	0.33	0.05
T_{blo}	Temp of engine block	−0.07	0.13	−0.06	0.31	0.05
H_{fac}	Conv coeff on flame face	−0.04	−0.07	0.12	0.28	0.04
H_{blo}	Conv coeff into engine block	0.09	—	−0.09	0.26	0.04
H_{int}	Conv coeff into intake valve	0.03	—	−0.03	0.04	0.01
Error					1.45	0.22
Total					665.98	

An example of the calculation of the sum of squares due to the factor in column four, H_{fac}, a three-level factor, follows:

$$SS_4 = 12(m_{4L}-m)^2+12(m_{4N}-m)^2 + 12(m_{4H}-m)^2 = 0.26. \quad (8)$$

The sums of squares for the other 13 factors are calculated in the same manner. Since an orthogonal array design matrix was used for this analysis, the following additive relationship exists between the various sums of squares [9],

$$SS_{Total} = \sum_{\text{all factors}} SS + SS_{error}. \quad (9)$$

The total sum of squares is given by

$$SS_{Total} = \sum_{i=1}^{36} \eta_i^2 - 36m^2 = 665.98. \quad (10)$$

Now the sum of squares due to error can be calculated since the other two terms in equation (9) are known,

$$SS_{error} = SS_{Total} - \sum_{\text{all factors}} SS = 665.98 - 664.53 = 1.45. \quad (11)$$

The sum of squares values for the 15 factors and the error are shown in Table 4. The factors are listed in order of decreasing influence. The total sum of squares is 665.98. Thus, the factor H_{blo} explains 0.04% of the overall variation in the temperature, the factor H_{fac} explains 0.04%, and the error explains 0.22%. The factors with the largest contribution to the total sum of squares have the greatest ability to influence the overall average temperature. Similar results for the other three locations of interest are shown in Norris [1].

3.3. *Results*

The first thing to note in the last column in Table 4 is that the contribution of the error to the total sum of squares is only 0.22%. This indicates that the simple additive model assumed in equation (1) was adequate, and while there are some interactions present, the effect is rather small when compared to main factor effects.

As can be seen from the last column in Table 4, the sum of squares values for the bulk fluid temperature, T_{flu}, dominates all other factors, and this was found to be true at all four locations of interest. These results indicate that an accurate measurement of the bulk fluid temperature is essential in order for accurate values for the convection coefficients to be identified from the matching procedure. For this experiment there was a rather high level of confidence in the bulk fluid temperature.

The next largest contributor to the total sum of squares is the injector sleeve temperature, T_{inj}, which accounts for only 0.64% of the total sum of squares. Notice, changing the injector sleeve temperature from 350 to 366 K results in only a 0.80 K change in calculated temperature at the nodal point located in the stagnant region. The next issue to address is the effect that a 0.80 K change in nodal temperature would have on the convection coefficient determined for the stagnant region as a result of the inverse analysis. Several trial ANSYS® runs were made, and it was determined that a change in nodal temperature of 0.80 K would correspond to a change of about 100 kW m^{-2} K^{-1} in the convection coefficient determined for

this zone, which was 384 kW m^{-2} K^{-1}. Thus, regardless of which injector sleeve temperature was used for the analysis, the conclusion (that nucleate boiling is present in the stagnant region) would be the same. The other boundary conditions have even less of an influence on the results of the matching procedure. In fact, all but three of the factors have sum of squares values less than the sum of squares of the error, indicating that the effects of these 12 factors cannot be distinguished from the error incurred by assuming the additive model and as already stated, this error is quite small.

By examining the results for all four nodal locations, as presented in Norris [1], the following observations are made. As previously noted, the bulk fluid temperature dominates the total sum of squares at all locations of interest. The only other variable which accounts for greater than 10% of the total sum of squares, at any of the four locations, is the temperature of the engine block, T_{blo}, which accounts for 21% of the variability in the temperature recorded in the recirculation region between cylinders on the upstream side. Thus, an accurate measurement of the temperature of the engine block is necessary to obtain a good estimate for the convection coefficient in this region. Unfortunately, a good estimate was not available from this experiment, hence the conclusions for this region are subject to question.

3.4. *Uniqueness*

As previously indicated, the assumption was made when identifying the convection coefficients that the temperature at each thermocouple location was affected solely by the assumed convection coefficient for the region in which the thermocouple was located. This assumption would assure that the converged upon solution is unique. To investigate the validity of this assumption a second matrix experiment was designed and an ANOM was conducted in a manner similar to that previously presented. The results of this analysis will be briefly discussed here and the details can be found in Norris [1].

For this investigation a very large 'experimental region' was defined with an upper limit for each convection coefficient of 825 kW m^{-2} K^{-1} and a lower limit of 8 kW m^{-2} K^{-1}. The results of this analysis indicate that even with such a large experimental region two primary conclusions can be drawn. First, the results of the analysis are not sensitive to the convection coefficients assumed for regions other than those identified as the four critical flow regions. Second, the temperature at each thermocouple location of interest is primarily dependent only on the adjustable convection coefficient for the region corresponding to the thermocouple location.

The second conclusion was overwhelmingly strong for all thermocouple locations other than the separation region. In the separation region, the sensitivity analysis revealed that the temperature is primarily affected by the convection coefficient assumed for this region, but that the convection coefficients assumed for the 'other' regions ('other' defined here as all regions other than the three remaining critical flow regions) also influence the results, to a lesser degree. These results indicate that so long as reasonable estimates can be generated for the flow regions of the cylinder head external to the critical flow regions, then the temperature in the separation region can be assumed to be purely a function of the convection coefficient for that region. Based on the results of the flow visualization study, the fluid remained steady in all areas other than the four critical areas identified, and hence the velocity estimates identified from this study should be more than adequate for the purposes of estimating the convection coefficients for these regions. This statistical analysis was essential in assuring that the solution is unique.

4. DISCUSSION AND CONCLUSIONS

A statistical method which utilizes an orthogonal array matrix design is presented. Admittedly, the author developed and implemented the statistical analysis only after the data had been collected from the engine experiment. However, it is very important to recognize the potential of this tool as a guide during the physical experimental design. It would have been possible to conduct this statistical analysis, using past experience as a guide for the selection of factor levels, before the engine experiments were performed. Had this been done, the researcher would have known exactly which boundary conditions most strongly affect the results of the inverse analysis. Efforts could have been focused on obtaining accurate estimates for the most influential boundary conditions, and the time, cost and energy expended on measuring many of the boundary conditions, which had little effect, could have been saved. The method presented here can serve as a guide during the experimental design procedure and can result in not only decreased uncertainty in results, but also in reductions in cost and experimental effort.

Acknowledgements—The author acknowledges financial and technical support from the Georgia Institute of Technology and Cummins Engine Company, Inc. Special thanks is given to Ph.D. advisor Bill Wepfer and Cummins Technical contact, Kevin Hoag.

REFERENCES

1. Norris, P. M., An investigation of coolant passage heat transfer in a diesel engine cylinder head. Ph.D. dissertation, Georgia Institute of Technology, Atlanta, Georgia, 1992.
2. Norris, P. M., Wepfer, W., Hoag, K. L. and Courtine-White, D., Experimental and analytical studies of cylinder head cooling. *Proceedings of the Vehicle Thermal Management Systems Conference*, 1993, pp. 423–429.
3. Norris, P. M., Hoag, K. L. and Wepfer, W., Heat transfer regimes in the coolant passages of a diesel engine

cylinder head. *Experimental Heat Transfer*, 1994, **7**, 43–53.
4. Finlay, I. C., Boyle, R. J., Pirault, J. P. and Biddulph, T., Nucleate and film boiling of engine coolants flowing in a uniformly heated duct of small cross section, SAE 870032, 1987.
5. Hoag, K. L. and Brasmer, S. E., The use of flow visualization and computational fluid mechanics in cylinder head cooling jacket development, SAE 891897, 1989.
6. Kayes, W. M. and Perkins, H. C., Forced convection, internal flow in ducts. In *Handbook of Heat Transfer Fundamentals*, 2nd edn, ed. W. M. Rohsenow *et al.* McGraw-Hill, New York, 1985.
7. Nozue, Y., Satoh, H., Umetani, S., Thermal stress and strength prediction of diesel engine cylinder head, SAE 830148, 1983.
8. Box, G. E. P., Hunter, W. G. and Hunter, J. S., *Statistics for Experimenters*. Wiley, New York, 1978.
9. Phadke, M. S., *Quality Engineering Using Robust Design*. Prentice-Hall, New Jersey, 1989.
10. Taguchi, G. and Konishi, S., *Orthogonal Arrays and Linear Graphs*. ASI Press, Dearborn, Michigan, 1987.